ACADEMIC PRESS

Available online at www.sciencedirect.com

SCIENCE DIRECT®

Journal of Magnetic Resonance 158 (2002) 86–98

JMR Journal of Magnetic Resonance

www.academicpress.com

A subband ARMA modeling approach to high-resolution NMR spectroscopy

Marc Tomczak* and El-Hadi Djermoune

Centre de Recherche en Automatique de Nancy, CRAN-UMR CNRS 7039, Université Henri Poincaré, Nancy 1, B.P. 239, 54506 Vandoeuvre-lès-Nancy Cedex, France

Received 12 March 2002; revised 27 June 2002

Abstract

In this paper, a low numerical complexity method for parameter estimation of damped exponential signals is proposed. It allows one to handle with free induction decay (FID) signals of "high complexity" containing hundreds of resonances and composed of more than 100,000 samples. At first, it is recalled that the model of a FID is a particular autoregressive moving-average (ARMA) process in which the AR part contains all useful spectral information. Then the AR parameters may be estimated, by solving the high-order Yule–Walker (HOYW) equations using a singular-value decomposition procedure. To deal with high complexity signals, a subband decomposition scheme is proposed. The filtering operation involved by the decomposition produces colored noise that makes the ARMA modeling approach even more essential. Using three real-world ^{13}C NMR signals, the results achieved by the subband ARMA approach are compared with those obtained using the Fourier transform and a deconvolution algorithm.

Keywords: High resolution methods; Linear prediction; ARMA modeling; Subband decomposition; Magnetic resonance spectroscopy

1. Introduction

For several years, the possibility of using high-resolution (HR) spectral estimators instead of Fourier transform (FT) has received considerable attention in the literature devoted to NMR. Different approaches have been proposed, including maximum entropy methods (MEM) [1], linear prediction (LP) methods [2–6], state space methods [7–9], and more recently the filter diagonalization method (FDM) [10,11]. Iterative approaches such as maximum likelihood methods have also been considered. Here we will limit our discussion to noniterative algorithms.

Even if rather good results have been reported in particular cases of signals with a moderate number of samples and components, natural limitations of these methods appear when attempting to process very long signals with large numbers of components. Indeed, in this case, the algorithms have to handle very large matrices that must be inverted and possible large order polynomial rooting, resulting in prohibitive calculation costs and memory capacities requested. With this in mind, one should consider the following observations. On the one hand, it is known that in order to achieve sufficient accuracy and spectral resolution, the number of parameters has to be chosen much larger than the actual number of resonances. In the particular case of LP methods, this over parameterization is partly due to the AR approximation of the actual model of the FID which can be shown to be a particular autoregressive moving-average (ARMA) process. Thus, taking this structure into account will help to limit the number of necessary parameters. However, this will obviously not be sufficient when dealing with FIDs of often more than 100,000 samples and composed of several hundreds of damped sinusoids. So, on the other hand, in such cases it would be wiser to perform a subband decomposition before the estimation process itself [12,13]. This enables one to transform a complex estimation problem into a

* Corresponding author.
E-mail addresses: marc.tomczak@cran.uhp-nancy.fr (M. Tomczak), el-hadi.djermoune@cran.uhp-nancy.fr (E.-H. Djermoune).

1090-7807/02/$ - see front matter © 2002 Elsevier Science (USA). All rights reserved.
PII: S1090-7807(02)00064-2

set of subproblems, each much simpler and more favorable from a numerical point of view. Moreover, it is known that such decomposition procedures may enhance the performances of the HR spectral estimator used [14,15].

In this framework, some local spectral analysis schemes have already been proposed in the NMR literature [16,17] and this idea still seems to be of interest in this community [18]. The reduction of calculation costs has been tackled from other points of view. For example, some authors proposed the use of fast LP algorithms [19]. Although such approaches actually allow one to use huge prediction orders, they are still inefficient to deal with signals of more than several thousands of samples. Moreover, the very large polynomial rooting involved in such situations becomes questionable.

In this paper, we propose an ARMA modeling of the FID, including a procedure for estimating the AR part of the ARMA process, used in combination with a subband decomposition, the latter being achieved by filtering and decimation operations. Unlike the LP-ZOOM approach [16], the method proposed performs a systematic decomposition of the whole spectral band without a priori information about the peaks location. Furthermore, the number of subbands being fixed, one can reasonably admit that each pseudo-FID (which is much shorter than the original FID), corresponding to the different subbands, contains fewer resonances so that the requested model order may be reduced in proportion. Accordingly, the number of roots to be determined will decrease too. On the whole, considering, say, 100 pseudo-FIDs, each being modeled by an order 100 model, will be roughly equivalent to processing the original FID with an order 10,000 but will not involve the same numerical difficulties.

The first part of the paper is devoted to the modeling of a sum of noisy damped sinusoids. It will be shown that the actual model of such a process can be viewed as an ARMA model in which all useful spectral information is contained in the AR part. Then a nonbiased estimator of the AR part, known as the HOYWSVD estimator [20], is presented. In the second part, the subband decomposition procedure is set forth. In particular, it will be shown that the pseudo-FID resulting from filtering and decimation operations may also be viewed as an ARMA process that may be estimated using the same algorithm as before. Finally, and after a brief summary of the complete method, the results achieved are compared with those obtained with a classical procedure. The latter, using a Fourier transform and a maximum likelihood deconvolution, will be named FT-MLD. In the case of ^{13}C experimental signals with more than a 100 components, the superiority of the approach proposed is pointed out.

2. Signal modeling and parameter estimation

2.1. Signal modeling

It is well established that the numerical signal $y(n)$ delivered by a spectrometer (generally an average signal rising from multiple measurements of the same experiment) can be represented by the following model

$$y(n) = \sum_{i=1}^{K} A_i e^{(\alpha_i + j2\pi f_i)nT + j\theta_i} + e(n) = x(n) + e(n) \tag{1}$$

for $n = 0, \ldots, N-1$. A_i is the amplitude, f_i the frequency, α_i the damping factor, and θ_i the phase of each of the K components. T is the sampling period and N is the total number of observations. The error term $e(n)$ is representative of measurement noise. It is usually assumed to be white noise. At any rate, the estimator presented below is able to handle colored noise of MA type.

The noise-free part of the signal, $x(n)$, admits the equivalent but more compact representation

$$x(n) = \sum_{i=1}^{K} h_i z_i^n, \tag{2}$$

where $h_i = A_i \exp(j\theta_i)$ and $z_i = \exp(\alpha_i + j2\pi f_i)T$. It can be established [21] that $x(n)$ can be written in a linear prediction form

$$x(n) = -\sum_{m=1}^{K} a(m)x(n-m) \tag{3}$$

with $a(0) = 1$ and where the parameters $a(m)$ are such that the terms z_i from Eq. (2) are the roots of the polynomial

$$\Phi(z) = \sum_{m=0}^{K} a(m)z^{K-m}. \tag{4}$$

This means in particular that all the frequency information of the noise-free signal is included in the $a(m)$ coefficients. Using Eq. (1), one can deduce the following relation from Eq. (3):

$$y(n) - e(n) = -\sum_{m=1}^{K} a(m)(y(n-m) - e(n-m)). \tag{5}$$

Thus

$$y(n) = -\sum_{m=1}^{K} a(m)y(n-m) + \sum_{m=0}^{K} a(m)e(n-m) \tag{6}$$

which, under the assumption of a white sequence $e(n)$, resembles an ARMA process. This particular process has, at first, the same coefficients for the AR and MA parts. Second, this is an unusual ARMA process because $e(n)$ figures an output noise instead of a driving noise. In fact, the process is generated by an impulse input which makes it nonstationary. Thus, it is actually

a limiting form of an ARMA process. But, what is important to note is that the autocorrelation function of the actual process will follow, as will be seen later, the same recurrence equations as an ARMA process. So, under certain conditions, it is possible to use the same estimation procedure as in the classical ARMA case. The process defined by Eq. (6) will be called the equivalent minimal ARMA representation of signal $y(n)$. This result is well known [22–24] but, curiously, the use of an ARMA technique in the estimation procedure has not received great attention in the NMR literature. In fact, most of the estimation methods in linear prediction, more or less, tend to approximate the ARMA process by an AR one. But for this approximation to hold sufficiently, the prediction order has to be chosen several times larger than the actual number of poles, thus leading to an overparameterized problem. Now, it is known that such an overparameterization is needed for the LP methods to yield sufficient spectral resolution, especially at low signal-to-noise ratio (SNR), whatever model is used. So, considering the actual ARMA structure permits one to reduce the total number of parameters to be estimated. Let us recall that the MA parameters need not be computed, which is preferable because of the nonlinear aspect of ARMA identification.

As a more general case, which will be useful in the discussion about subband modeling, one can also consider the case of colored noise, that is a MA noise sequence of order M

$$e(n) = \sum_{i=1}^{M} c(i)\epsilon(n-i), \tag{7}$$

where $\epsilon(n)$ is a white sequence. Now the signal $y(n)$ is described by a minimal ARMA$(K, K+M)$ process of the form

$$y(n) = -\sum_{m=1}^{K} a(m)y(n-m) + \sum_{m=0}^{K+M} b(m)\epsilon(n-m). \tag{8}$$

Here again, it must be noticed that the frequency information of the noiseless signal remains in the AR part of the ARMA process.

2.2. Nonbiased estimation of the AR part of an ARMA process

In the previous section, it has been shown that the problem is now to estimate the AR part of an ARMA process to get access to frequency information. One approach to make a nonbiased estimation of solely the AR part is the so-called high-order Yule–Walker (HOYW) estimator [20,25], which is strongly related to another estimator called the overdetermined instrumental variable with delayed observations [26]. Because of its better numerical properties, we finally chose a particular HOYW estimator, called HOYWSVD due to the singular-value decomposition (SVD) of the shifted autocorrelation matrix it involves. This approach is similar to LPSVD but operates on the autocorrelation sequence rather than on the data samples. Another notable difference lies in the fact that the corresponding autocorrelation matrix may be shifted to remove the noise influence, thus leading to an unbiased AR estimation.

The principle of this estimation procedure is now briefly recalled. Starting with a standard ARMA process of the form

$$u(n) = -\sum_{m=1}^{p} a(m)u(n-m) + \sum_{m=0}^{q} b(m)e(n-m), \tag{9}$$

it is well known [27] that

$$r(m) = -\sum_{i=1}^{p} a(i)r(m-i), \quad m \geqslant q, \tag{10}$$

where $r(m) = E[u^*(n)u(n+m)]$ is defined as the autocorrelation sequence of $u(n)$. Rewriting Eq. (10) for $q \leqslant m \leqslant q+p$ yields the so-called modified Yule–Walker equations. In the case where $q \leqslant m \leqslant q+c,\ c > p$, the overdetermined Yule–Walker equation system is obtained. Moreover, if the order p is greater than the actual order of the AR part, we get the HOYW equations that have the general form

$$\bar{\mathbf{R}} \cdot \mathbf{a} = -\bar{\mathbf{r}}, \tag{11}$$

where $\bar{\mathbf{R}}$ is a $c \times p$ matrix and $\bar{\mathbf{r}}$ a $c \times 1$ vector of autocorrelations. The vector $\mathbf{a}$ contains the AR coefficients.

In the case of process defined by Eqs. (1) and (6), it can be shown that the autocorrelation function is given by

$$r_n(m) = \sum_{i=1}^{K} h_i'(n) z_i^m + \sigma^2\delta(m), \tag{12}$$

where $h_i'(n) = h_i z_i^n \sum_{j=1}^{K} h_j^* z_j^{*n}$ and σ^2 is the variance of $e(n)$. Note that, in this case, the autocorrelation function is time-dependent but it satisfies a recurrence of the same form as in Eq. (10) for all time indexes n

$$r_n(m) = -\sum_{i=1}^{K} a(i)r_n(m-i), \quad m > K. \tag{13}$$

Clearly, a set of equations similar to Eq. (11) may then be established:

$$\mathbf{R} \cdot \mathbf{a} = -\mathbf{r}. \tag{14}$$

Since the autocorrelation sequence is unknown, it has to be estimated from the FID signal samples. Depending on the autocorrelation estimator used, the equation above becomes

$$\hat{\mathbf{R}} \cdot \mathbf{a} \approx -\hat{\mathbf{r}}, \tag{15}$$

where

$$\hat{\mathbf{R}} = \begin{pmatrix} \hat{r}(1,q+1) & \hat{r}(2,q+1) & \dots & \hat{r}(p,q+1) \\ \hat{r}(1,q+2) & \hat{r}(2,q+2) & \dots & \hat{r}(p,q+2) \\ \vdots & \vdots & & \vdots \\ \hat{r}(1,q+c) & \hat{r}(2,q+c) & \cdots & \hat{r}(p,q+c) \end{pmatrix},$$

and

$$\hat{\mathbf{r}} = [\hat{r}(0,q+1), \hat{r}(0,q+2), \dots, \hat{r}(0,q+c)]^{\mathrm{T}}.$$

Here $\hat{r}(i,j)$ will correspond to different autocorrelation estimators, depending on the summation horizon [22]. Integer q must be at least equal to K in the case of white noise and to $K+M$ in the case of colored noise. Note that, in practice, oversizing the order p (i.e., $p > K$) actually improves resolution [21,22,28]. In the particular case of narrowband signals, further improvements are observed if the overdetermination factor c is chosen large enough (see, e.g., [29]).

Given an estimate of the autocorrelation, the AR parameters can be computed in the same manner as in the LPSVD method in which the signal matrix is replaced by the autocorrelation matrix. The SVD-based solution of the HOYW equations is given by

$$\hat{\mathbf{a}} = -\hat{\mathbf{R}}^{\#}\hat{\mathbf{r}} = -\mathbf{V}\mathbf{S}^{\#}\mathbf{U}^{H}.\hat{\mathbf{r}}, \tag{16}$$

where $\hat{\mathbf{R}} = \mathbf{U}\mathbf{S}\mathbf{V}^{H}$ is the singular-value decomposition of matrix $\hat{\mathbf{R}}$. The reduced rank Moore–Penrose pseudoinverse $\mathbf{S}^{\#}$ is obtained by inverting the first $\hat{K}$ largest singular values and setting the others to zero. Here, $\hat{K}$ is an estimation of K, the real number of damped sinusoids.

Once the AR parameters are obtained, frequencies and damping factors correspond to the imaginary and real parts of the logarithm of the AR polynomial roots, respectively. The complex amplitudes may be estimated by another least-squares procedure using Eq. (1).

Due to the decaying feature of FID signals, the results obtained by the HOYWSVD technique depend closely on the choice of the autocorrelation estimator. From a linear prediction theory point of view, there are five common estimators called *prewindowed*, *postwindowed*, *autocorrelation*, *covariance*, and *modified covariance* estimators [21]. When processing damped exponentials in reverse time order (or growing exponentials in a normal sense), the postwindowed estimator is not well-suited because the nonobserved points that come at the end of the signal are inherently assumed to be equal to zero. The autocorrelation estimator, which corresponds to the classical case of the Yule–Walker equations [27], implies pre- and postwindowing of the data. For this reason, it is known to yield less resolution, particularly for short signals, and what is more, it ensures the stability of the model, even in backward prediction. Now, it will be seen in the next section that this property is undesirable. Because it involves forward and backward prediction, the modified covariance estimator is better suited to undamped complex exponentials. The covariance estimator is a quite good candidate but the prewindowed one is preferred since it operates on more samples. The prewindowed estimator is given by

$$\hat{r}(i,j) = \frac{1}{N}\sum_{k=\max(i,j)}^{N} y(k-i)y^{*}(k-j). \tag{17}$$

This estimator implies that the points after the end of the signal are zero which is in concordance with the damped feature of the FID, and what is more, it can be shown to satisfy Eq. (13).

2.3. Estimation of the number of components

At this point, the important question of the estimation of the number of components has not been addressed. This problem may be seen as a problem of separation of two subspaces, one being the signal subspace and the other the noise subspace. Ideally, $\hat{K}$ should be equal to the dimension of the signal subspace, i.e., the real number of components K. The most common estimators of the number of components are AIC and MDL [30,31]. Both estimators work using the SVD of the autocorrelation matrix and thus do not require major additional calculations.

We have seen before that, as for the noise-free signal $x(n)$, the autocorrelation sequence of the noisy signal $y(n)$ could be represented by a linear prediction difference equation. This is also true for the autocorrelation sequence of $y(n)$ considered in chronological reverse order, but it must be noted that in this case, the model is unstable; thus the corresponding poles lie outside the unit circle. The well-known unit circle criterion (UCC), which is intended to help to separate the signal poles from extraneous ones, is based upon this property [32]. In order to preserve it when the estimated autocorrelation is used instead of the true autocorrelation sequence, autocorrelation estimators that ensure the model stability must be excluded. Thus, only the covariance and the prewindowed estimators may be used in our case. When using HOYWSVD, associated with the prewindowed autocorrelation estimator, with $p > K$, the $p-K$ additional zeros of the prediction polynomial tend to stay inside the unit circle when those associated with the signal lie outside. We have seen in simulations that if the number of components is slightly overestimated, UCC still returns the good number of signal poles (number of zeros lying outside the unit circle). So, the UCC enables one to correct possible errors made by the estimator of the number of components, provided that the latter is not underestimated.

Note that particular order estimators, well suited to the HOYW ARMA modeling problem, have been proposed [24,33]. But, for the sake of generality, we only considered the well-known MDL criterion. Anyhow, it must be admitted that the estimator of the number of

components may have poor performances when the number of spectral lines is too large. Now, the method we propose later is based on a subband decomposition. When performing the decomposition, it is possible to choose the size of subbands so that the corresponding numbers of components to be processed are limited enough.

3. A subband decomposition approach

3.1. Introduction and motivations

The concept of subband decomposition, based on an operation called *filtering and decimation* (FD), is very familiar to the members of the signal processing community who use it in various situations [34]. In the particular domain of spectral analysis, it has been used for years in association with the FT in order to produce a zoom effect on specific spectral bands. It should be clearly recalled that in this case, no real frequency resolution improvement is achieved.

However, since the work of Quirk and Liu [14], it has been known that such an improvement actually arises with parametric estimators. Other arguments are in favor of this approach of spectral analysis, and many papers have been published on the subject (see, e.g., [15,35]). Some of the methods proposed are adaptive insofar as the decomposition is carried on according to the spectral contents of the signal under study [36]. Here we will consider a nonadaptive decomposition scheme. In the NMR framework, the concept of local spectral analysis was originally introduced by Tang and Norris [16]. Since this early work, to our knowledge, this matter has only seen a few new contributions [17,18,37]. As was said before, the concept of subband decomposition allows one to generalize the local spectral analysis on the whole bandwidth. Moreover, it simplifies considerably the initial estimation problem and thus seems to be well adapted to the NMR context because of the high complexity of the signals encountered. The spectral decomposition is achieved by multiple FD operations. But it will be seen that the filtering involved has a notable influence on the underlying process modeling.

3.2. Subband decomposition fundamentals

3.2.1. Decimation

We consider only the case of decimation by an integer d called the decimation factor. The decimated version of signal $s(n)$ is defined as

$$s_d(n) = s(dn). \tag{18}$$

Such an operation may be regarded as a new sampling of the initial signal. It can be shown [34] that the FT of $s_d(n)$ is expressed as

$$S_d(\mathrm{e}^{j\omega}) = \frac{1}{d}\sum_{k=0}^{d-1} S(\mathrm{e}^{j(\omega-2\pi k)/d}). \tag{19}$$

This shows that the FT of the decimated signal is a superposition of d enlarged and shifted versions of the original FT.

3.2.2. Filtering and decimation

As in all sampling operations, it is necessary to proceed with a bandpass prefiltering of the signal to be decimated, in order to avoid aliasing phenomena. More precisely, the maximal signal's bandwidth before decimation is $\Delta\omega = 2\pi/d$. To obtain a complete subband decomposition of signal $s(n)$, a uniform filter bank may be used as depicted in Fig. 1.

A filter is defined by its transfer function

$$G(z) = \sum_{k=-\infty}^{\infty} g_k z^{-k}, \tag{20}$$

where the g_k are the coefficients of the filter impulse response. Henceforth, the time-domain relationship between the filtered and decimated signal $f(n)$ and the original signal $s(n)$ is

$$f(n) = \sum_{k=-\infty}^{\infty} s(k)g_{dn-k} = \sum_{k=-\infty}^{\infty} s(dn-k)g_k. \tag{21}$$

In the structure of Fig. 1, each filter $G_m(z)$ is a shifted version of the basic filter $G_0(z)$; the latter will be denoted $G(z)$ for simplicity. Thus, we have

$$G_m(z) = G(z\mathrm{e}^{-j2\pi m/d}), \quad m = 1,\ldots,d-1. \tag{22}$$

The same result can indeed be achieved by always using the same lowpass filter but adequately modulating the initial signal. It is clear that in practice, nonideal filters have to be used. This results in some problems that are to be discussed later.

3.3. Modeling of pseudo-FIDs

The question is now to determine the adequate model for each subsignal or pseudo-FID stemming from the FD operations. We begin with the original signal $y(n)$

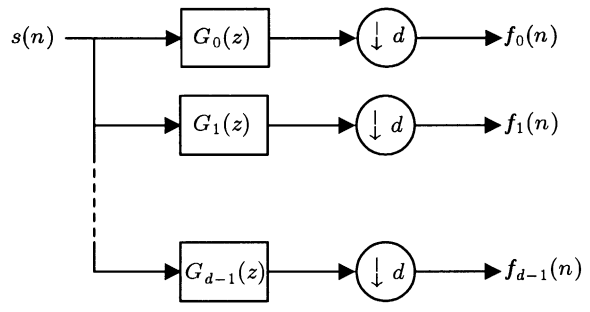

Fig. 1. The overall subband decomposition scheme.

defined in Eq. (1). At first, the signal is modulated at a frequency f_m $(m = 0, 1, \ldots, d-1)$ corresponding to the bandwidth central frequency of the mth filter of transfer function $G_m(z)$

$$y_m(n) = y(n)\mathrm{e}^{-j2\pi n f_m}. \tag{23}$$

As we already mentioned, this enables one to use a unique low-pass filter $G(z)$. So, we can now, without loss of generality, consider the special case when $f_m = 0$; i.e. $y_m(n) = y(n)$.

Then the signal is filtered with a finite impulse response (FIR) filter $G(z)$ of order L. The filtered signal, denoted by $y'(n)$, is given by the discrete convolution

$$y'(n) = \sum_{k=0}^{L} g_k y(n-k). \tag{24}$$

This signal is composed of $N - L$ samples, because the first L transitory points are suppressed. Using Eqs. (1) and (2), it follows after straightforward calculation [35]:

$$\begin{aligned} y'(n) &= \sum_{i=1}^{K} h_i G(z_i) z_i^L z_i^n + \sum_{k=0}^{L} g_k e(n-k) \\ &= \sum_{i=1}^{K} h_i G(z_i) z_i^L z_i^n + e'(n). \end{aligned} \tag{25}$$

The effects of the FIR filtering are to scale the complex amplitudes and to color the noise. In practice, the filter is indeed nonideal, but it seems reasonable to admit that a portion $K - K'$ of the components, located outside the filter bandwidth, are sufficiently attenuated to be assimilated to a supplementary noise term noted $v'(n)$

$$\begin{aligned} y'(n) &= \sum_{i=1}^{K'} h_i G(z_i) z_i^L z_i^n + \sum_{i=K'+1}^{K} h_i G(z_i) z_i^L z_i^n + e'(n) \\ &= \sum_{i=1}^{K'} h_i' z_i^n + v'(n) + e'(n), \end{aligned} \tag{26}$$

where

$$h_i' = h_i G(z_i) z_i^L. \tag{27}$$

Now, consider the decimation stage. Starting from $y'(n)$, it is possible to obtain a set of different, decimated series, named polyphasic series

$$y'_{d,\eta}(n) = y'(dn + \eta), \quad \begin{cases} n = 0, 1, \ldots, N' \\ \eta = 0, 1, \ldots, d-1, \end{cases} \tag{28}$$

where $N' = [(N-L)/d]$ represents the length of the decimated series ($[x]$ stands for the integer part of x). In this paper we make use of only the first series, that is for $\eta = 0$.

Finally, the filtered and decimated signal (pseudo-FID) can be written

$$y'_d(n) = \sum_{i=1}^{K'} h_i' z_i'^n + v'_d(n) + e'_d(n), \tag{29}$$

where $v'_d(n) = v'(dn)$, $e'_d(n) = e'(dn)$ and

$$z_i' = z_i^d. \tag{30}$$

For reasons that have been exposed in [35], under certain conditions, the term $v'_d(n)$ and the bias it could introduce may be neglected. This is generally true if the filter transition band is sharp enough. Now, our model of the pseudo-FID reduces to

$$y'_d(n) = \sum_{i=1}^{K'} h_i' z_i'^n + e'_d(n). \tag{31}$$

Since $e'_d(n)$ is a resampled version of the MA(L) process $e'(n)$, it can be shown that $e'_d(n)$ is a MA($[L/d]$) process [38]. Now, the signal $y'_d(n)$ is a superposition of K' weighted complex exponentials and of the MA noise $e'_d(n)$. Thus, $y'_d(n)$ can be seen as a minimal ARMA $(K', K' + [L/d])$ process. Whenever the initial noise is a MA(M) process, then $e'_d(n)$ is a MA($[(L+M)/d]$) process. It is important to note that if more than one FD stage are needed, the additive noise is no longer white; this makes the AR-based estimators even more inadequate. Since the pseudo-FID is of the same type of that of Eq. (1), the HOYWSVD approach is still valid to estimate the frequencies via the AR parameters.

3.4. The decimation filter

As was pointed out before, the filter considered is a FIR one. Infinite impulse response (IIR) filters have not been retained for different reasons, among which include stability problems when small bandwidths are needed. The choice of a particular FIR filter seems not to be of crucial importance. A typical low-pass filter has two important features: the cut-off frequency ω_p and the stopband frequency ω_s. To avoid aliasing due to decimation, ω_s must verify the inequality

$$\omega_\mathrm{s} \leqslant \pi/d. \tag{32}$$

The filter being nonideal, the signal peaks located inside the transition band $[\omega_\mathrm{p}, \omega_\mathrm{s}]$ may be severely reduced; moreover, their variance is undoubtedly greater than for the peaks inside the bandpass. To overcome this problem, the signal poles estimated in the transition band should be eliminated, thus leading to the successive filters overlapping, as shown in Fig. 2, to retrieve all spectral information. This results in making the initial number of subbands increase from d to d'. As a consequence, the bandpass of the filter is now defined as $\omega_\mathrm{p} = \pi/d'$, where d' is greater than d. For simplicity, one can choose $d' = 2d$, so

$$\begin{aligned} &\omega_\mathrm{p} = \pi/2d, \\ &\omega_\mathrm{p} < \omega_\mathrm{s} \leqslant \pi/d. \end{aligned} \tag{33}$$

It must be mentioned that for high values of the decimation factor d, the filter involves several hundreds of

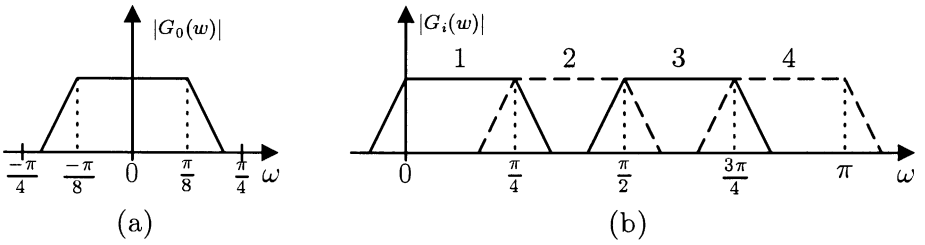

Fig. 2. (a) Decimation filter; (b) overlapping decimation filters for $d = 4$ ($\omega_p = \pi/8$ and $\omega_p < \omega_s \leqslant \pi/4$). Four subbands in the frequency interval $[0, \pi]$ result from the decomposition.

coefficients, resulting in prohibitive filtering durations. In that particular case, an interpolated finite impulse response (IFIR) approach may be advantageously carried out [34]. Briefly, it consists in replacing the one-step FD(d) operation by successive FD(d_i) stages, where $d = \Pi_i d_i$ and the filters involved are much more simple. This allows one to drastically reduce the number of calculations.

3.5. The complete method (SB-HOYWSVD)

The method proposed may be briefly summarized as follows.

1. Choose factor d (which depends on the number of data samples and the complexity of the signal); then deduce the features of the filter using Eqs. (33).
2. Fix the operating parameter p; then put $q \approx p + [L/d]$. The parameter c should be at least equal to p.
3. For $m = 0, 1, \ldots, d' - 1$, repeat the following:
   (a) Generate a pseudo-FID by modulating the original signal (Eq. (23)) followed by a low-pass filtering and decimation.
   (b) Reverse the chronological order of the pseudo-FID; then perform a HOYWSYD estimation of the forward prediction coefficients using Eq. (16).
   (c) Perform a polynomial rooting of the forward prediction polynomial to find the signal poles; then select those lying outside the unit circle and reflect them inside to get the $\hat{z}_i'$'s.
   (d) Compute the subband complex amplitudes $\hat{h}_i'$.
   (e) Discard all poles outside the filter's bandpass.
4. Obtain the different fullband parameters (h_i, z_i) from the subband parameters (h_i' and z_i') using Eqs. (30) and (27).

Note that the frequencies, damping factors, amplitudes, and phases can be obtained directly from the parameters z_i and h_i.

4. Experimental results

In this section, some results obtained on experimental NMR signals are presented to demonstrate the usefulness of the subband ARMA estimation method. The results are compared to those obtained by a classical method (FT-MLD) and the ARMA estimation performed in the fullband (HOYWSYD). The FT-MLD method associates a classical FT approach with a maximum likelihood deconvolution (MLD) algorithm [39]. Here, this approach is used in the best possible conditions; that is, it makes use of the entire signal and, during the deconvolution process, the exact number of components K (which is perfectly known) is used. Hence, the FT-MLD algorithm is considered as the reference method for our trials. Note that K being known, the use of adapted thresholds allowed us to insist on the presence of some lines and to eliminate all supplementary ones, which is generally not possible in practice.

Three experimental signals, named NMRi ($i = 1, 2, 3$), are used. All of them were recorded on a Brucker AM 400 spectrometer (^{13}C frequency observation: 100.62 MHz). The signals are real of length 131,072 samples and were obtained using 1000 accumulations. Their chemical compositions are shown in Table 1. The first signal is of a low spectral complexity: it contains only nine, relatively spaced, components. The signals NMR2 and NMR3 whose absorption spectra are shown in Fig. 3 are more intricate because they contain many more components, generally very close one to the other (especially NMR3 signal).

For the subband approach, the decimation factor to be used depends on the problem complexity (number of components) and on the number of samples. Here, it was fixed to ensure good operating conditions, that is to have at once pseudo-FIDs of reasonable length and a sufficient reduction of the number of parameters that have to be estimated simultaneously. For example, if we chose to have 1000 samples of pseudo-FIDs, the decimation factor has to be fixed to $d = 128$ (and $d' = 256$). This tuning has been retained for all the trials presented below. The decimation filter is then designed using the IFIR approach, which results in actually operating five Kaiser filters of respective orders 16, 17, 10, 12, 39 and successive decimation stages with decimation factors of 4, 4, 2, 2, 2. With these parameters, each subsignal contains $N' = 1001$ data samples. Since the number of components lying in a particular subband is not known, it is estimated using the MDL criterion.

Table 1
Chemical compositions corresponding to signals NMR1-3

Signal	Products	Formulae	Quantity (g)
NMR1	Ethylbenzene	C_8H_{10}	—
	Chloroform	$CDCl_3$	—
NMR2	Benzene	C_6H_6	0.0362
	Ethylbenzene	C_8H_{10}	0.2818
	Toluene	C_7H_8	0.5195
	1,3-Dimethylbenzene	C_8H_{10}	0.2449
	1,3-Dimethyl-5-ethylbenzene	C_8H_{14}	0.4002
	Chloroform	$CDCl_3$	—
NMR3	Toluene	C_7H_8	0.5322
	meta-Ethyltoluene	C_9H_{12}	0.3395
	Ethylbenzene	C_8H_{10}	0.3931
	o-Xylene	C_8H_{10}	0.2986
	1,3-Dimethyl-5-ethylbenzene	$C_{10}H_{14}$	0.2651
	m-Xylene	C_8H_{10}	0.3089
	Tetraline	$C_{10}H_{12}$	0.3312
	Indane	C_9H_{10}	0.2893
	n-Propylbenzene	C_9H_{12}	0.1593
	p-Xylene	C_8H_{10}	0.1208
	1,2-Dimethyl-3-ethylbenzene	$C_{10}H_{14}$	0.1150
	1,3,5-Trimethylbenzene	C_9H_{12}	0.0806
	Naphthalene	$C_{10}H_8$	0.0188
	1,2,3-Trimethylbenzene	C_9H_{12}	0.0488
	Isobutylbenzene	$C_{10}H_{14}$	0.0132
	Benzene	C_6H_6	0.0765
	2,4-Dimethylhexane	C_8H_{18}	0.1012
	2,3,4-Trimethylpentane	C_8H_{18}	0.1489
	TMS	$C_4H_{12}Si$	—
	Dioxane	$C_4H_8O_2$	—
	Chloroform	$CDCl_3$	—

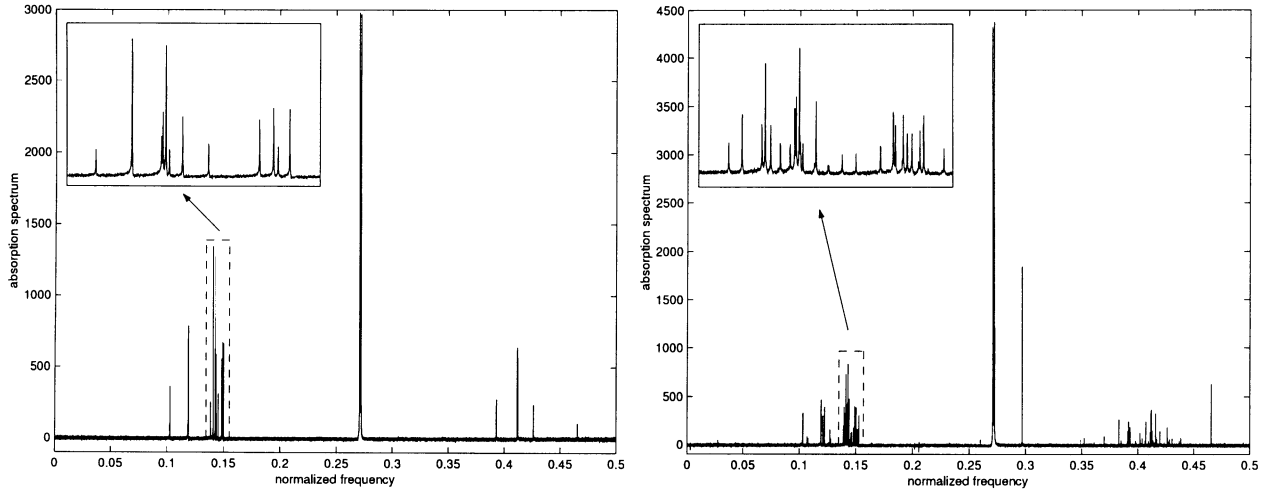

Fig. 3. Absorption spectra of experimental signals: (a) NMR2 and (b) NMR3.

4.1. First experimental signal: NMR1

The first signal NMR1 comes from experiments made on a solution of ethylbenzene in deuterated chloroform $CDCl_3$ (1 M/l). It contains nine components in the positive frequency interval $[0, \pi/2]$. The time between consecutive pulses was set to 1 s. With this signal, the principal difficulty (although it is of little interest) is to resolve the three central peaks between 0.25 and 0.3 Hz (lines 5, 6, and 7 of Table 2) due to the presence of chloroform.

The results achieved on the signal using the HOYWSVD technique (i.e., in the fullband) are shown in

Table 2
Results achieved on signal NMR1

Line	FT-MLD		HOYWSVD		SB-HOYWSVD	
	f	A	f	A	f	A
1	0.10269	0.120	0.10269	0.093	0.10269	0.119
2	0.14276	1.000	0.14276	1.000	0.14277	1.000
3	0.14391	0.950	0.14390	0.792	0.14391	0.948
4	0.14960	0.548	0.14960	0.483	0.14961	0.476
5	0.27099	0.197	0.27093	0.354	0.27099	0.179
6	0.27178	0.204	—	—	0.27179	0.185
7	0.27258	0.206	0.27278	0.140	0.27259	0.194
8	0.39283	0.612	0.39283	0.398	0.39283	0.559
9	0.42627	0.784	0.42627	0.504	0.42628	0.648

Table 2. Due to hardware limitations, only 8192 samples of the 131,072 are used. After some tests, the parameters p, q, and c are set to 300, 400, and 800, respectively. The truncation number $K = 18$ is assumed to be known. With these parameters, eight of the nine theoretical components are detected, while line 6 failed to be detected.

With the subband technique using much lower ARMA orders ($p = 10$, $q = 30$, $c = 80$), all the components have been detected, although their number was unknown. Note that the decimation factor used for this example is high regarding the spectral content of the signal. As a matter of fact, comparable results may be achieved with $d = 32$. Concerning the amplitude estimation, it can be seen that the results are rather poor with the HOYWSVD approach while the amplitudes estimated by FT-MLD and SB-HOYWSVD are comparable. It may be noted that the amplitude of line 5 is overestimated by HOYWSVD, due to the missing line 6. Indeed, this amplitude corresponds roughly to the sum of the amplitudes of lines 5 and 6. Calculation times were observed to be of 30 s for HOYWSVD (on 8192 samples) and 1 min 23 s for SB-HOYWSVD (on the whole signal) on a 800 MHz PC and under a Matlab environment. Note that in the case of SB-HOYWSVD, filtering time was 1 min.

4.2. Second experimental signal: NMR2

The second experimental signal NMR2 corresponds to a more intricate situation, that is a mixture of five compounds with known concentrations $CDCl_3$. The quantitative recording is based on the addition of a relaxation agent that shortens the longitudinal relaxation time T_1; the time between consecutive pulses was therefore set to 35 s. There are 28 spectral lines, some of them being extremely mixed up and thus overlapping. We focus our attention on this particular zone, named NMR2A, around relative frequency 0.143 Hz. The operating parameters p, q, and c of the HOYWSVD method are set to 600, 600, and 800, respectively. The algorithm makes use of only the first 8128 samples. As for signal NMR1, the truncation number is set to the theoretical number of components (i.e., $K = 56$). Despite this, this method fails to detect 14 components and finds only one peak among 5 in NMR2A. In contrast, the same method applied in subband with $p = 30$, $q = 50$, $c = 120$ succeeds in detecting all of the spectral lines with estimated amplitudes approximately equal to those obtained by the FT-MLD method. See Table 3 for the results achieved on NMR2A zone.

Here we see that in a situation of average complexity, the HOYWSVD method requires large model orders and, when this is not true, it fails to detect all the components. On the other hand, the SB-HOYWSVD method detects all the components with relatively low model orders. The HOYWSVD took 1 min 30 s in order to process the first 8192 samples while SB-HOYWSVD dealt with the 128k samples in 1 min 41 s.

Table 3
Results achieved on signal NMR2 in the NMR2A zone

Line	FT-MLD		HOYWSVD		SB-HOYWSVD	
	f	A	f	A	f	A
...	...	...	...	...	...	...
8	0.14259	0.032	—	—	0.14260	0.028
9	0.14268	0.055	—	—	0.14269	0.066
10	0.14285	0.115	—	—	0.14287	0.136
11	0.14307	0.024	—	—	0.14308	0.027
12	0.14385	0.051	0.14392	0.147	0.14386	0.063
...	...	...	...	...	...	...

4.3. Third experimental signal: NMR3

The signal NMR3 results from quantitative experiments on a synthesized mixture of 19 compounds in $CDCl_3$, with tetramethylsilane (TMS) as the internal reference. Hence the complete chemical composition and the chemical shifts (δ/TMS) of the lines of the individual products are known. Some of them are shown in Table 4. Toluene being the most concentrated compound, two lines corresponding to the equivalent carbons, C6–C2 (32nd line) and C3–C5 (38th line), have the maximal intensity. The latter is therefore set to 100% and, from the theoretical composition, the intensities of the other lines are expressed as a percentage of these reference lines. The deconvolution is done with $K = 104$ a priori known, which, of course, is an advantage. For this example, the

Table 4
Results achieved in subbands 27, 37, 39, and 70 of signal NMR3

Band	Line	Theoretical[a]		FT-MLD[b]		SB-HOYWSVD[c]	
J	L	δ (ppm)	I (%)	f	A (%)	f	A (%)
...	...	...	...	...	...	...	...
	6	144.26	32.05	0.10277	32.87	0.10277	34.87
27	7	144.23	24.45	0.10286	46.39	0.10286	44.31
	8	144.22	17.10	—	—	—	—
	9	144.06	42.38	0.10303	41.28	0.10303	40.92
...	...	...	...	...	...	...	...
	31	129.11	43.37	0.14073	42.02	0.14073	41.88
	32	129.06	100.00	0.14092	100.00	0.14092	100.00
	33	128.94	39.40	0.14124	40.16	0.14124	44.53
	34	128.72	24.45	0.14181	25.25	0.14181	25.99
	35	128.47	22.98	0.14239	21.27	0.14239	20.57
	36	128.37	50.86	0.14267	51.20	0.14266	52.06
37	37	128.31	64.11	0.14275	66.86	0.14275	61.54
	38	128.25	100.00	0.14293	65.22	0.14293	94.19
	39	128.23	22.98	0.14297	75.81	0.14296	34.53
	40	128.23	24.45	0.14301	12.94	0.14301	29.07
	41	128.15	25.19	0.14315	23.62	0.14315	25.92
	42	128.07	1.70	—	—	—	—
	43	127.88	5.08	0.14382	8.24	0.14381	7.46
	44	127.86	64.11	0.14392	64.67	0.14392	64.41
...	...	...	...	...	...	...	...
	50	126.06	50.38	0.14848	48.29	0.14848	47.19
	51	126.03	7.42	0.14851	19.03	0.14851	27.34
	52	125.95	42.38	0.14861	41.50	0.14861	44.22
	53	125.81	5.08	0.14902	6.43	0.14903	2.01
	54	125.80	48.70	0.14907	48.10	0.14906	55.16
	55	125.72	34.20	0.14931	33.63	0.14931	33.47
39	56	125.63	11.49	—	—	—	—
	57	125.62	0.85	—	—	—	—
	58	125.59	32.05	0.14958	48.34	0.14958	50.67
	59	125.45	7.42	0.14996	6.64	0.14996	8.30
	60	125.38	43.37	0.15006	39.10	0.15006	38.66
	61	125.33	50.00	0.15028	48.13	0.15028	49.36
	62	125.23	3.52	—	—	0.15052	3.62
	63	124.85	24.45	0.15146	24.60	0.15146	25.78
...	...	...	...	...	...	...	...
	72					0.27026	1.02
	73	77.30		0.27064	1923.5	0.27063	2012.26
70	74					0.27086	10.77
	75	77.00		0.27143	1914.9	0.27143	2003.53
	76					0.27151	11.99
	77	76.70		0.27223	1961.9	0.27223	2038.43
...	...	...	...	...	...	...	...

[a] Theoretical lines with corresponding chemical component, chemical shifting (in ppm), and relative intensity (%) with respect to toluene's 32nd line (denoted by L_{32}).

[b] Results of the FT-MLD approach: estimated normalized frequencies and estimated relative intensities (directly calculated from estimated amplitudes).

[c] Results achieved by the SB-HOYWSVD method.

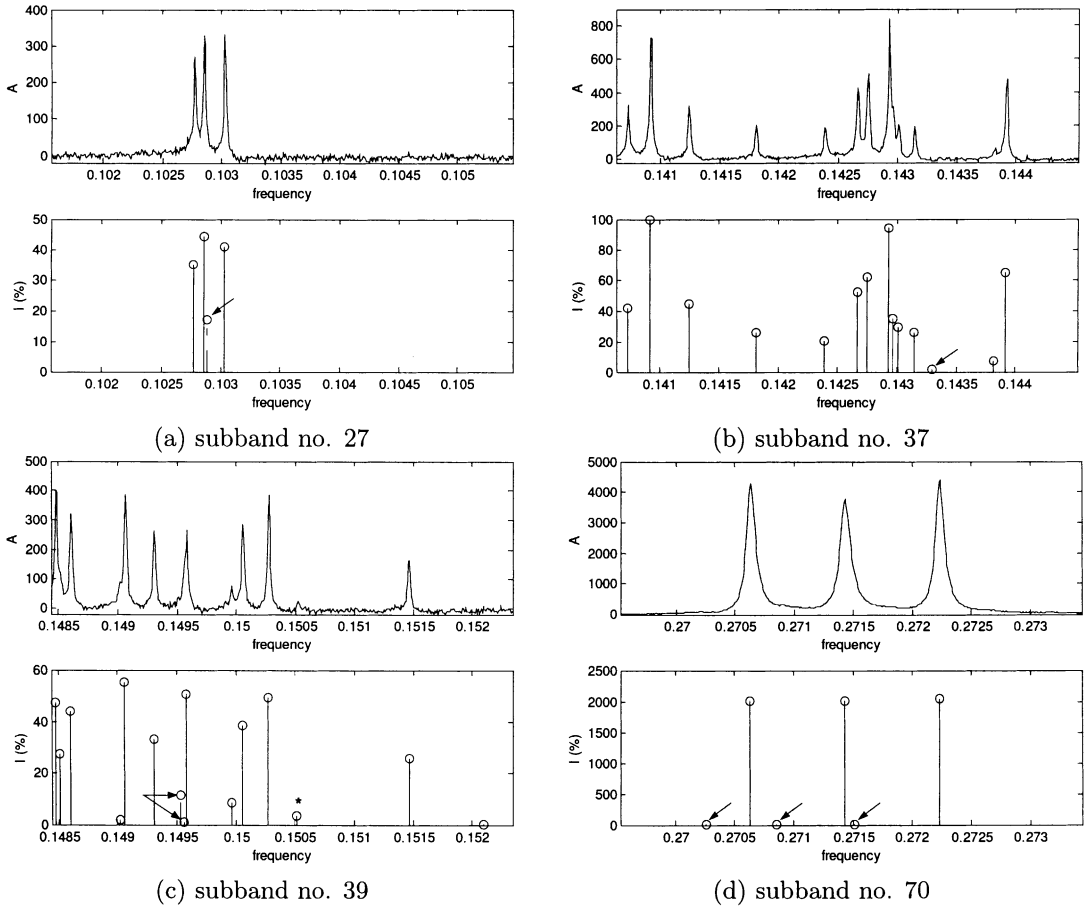

Fig. 4. Results achieved on some subbands of signal NMR3. Arrows point out nondetected components in subbands 27 (a), 37 (b), 39 (c), and spurious ones in subband 70 (d). The star indicates what line is detected by SB-HOYWSVD and missed by FT-MLD.

HOYWSVD methods has not been considered because of its great lack of performance. The parameters of the SB-HOYWSVD approach are $p = 80, q = 100, c = 160$. The results obtained by the two methods, FT-MLD and SB-HOYWSVD, are compared in Table 4 together with the theoretical line spectrum. Some subbands (numbered by J) $J = 27, 37, 39$, and 70 are depicted in Fig. 4. Each subfigure shows the FT absorption spectrum together with the line spectrum estimated by SB-HOYWSVD.

With the aforementioned parameters, the SB-HOYWSVD method detects 118 lines among which 94 correspond to actual theoretical lines, and 24 seem to have no theoretical correspondent. Ten theoretical lines are not detected. The FT-MLD made only 93 good detections and missed 11 theoretical lines, despite the use of the correct number of components.

Concerning the 10 lines not retrieved by the subband approach, two different situations may be distinguished: nondetection of eight peaks with very small amplitudes (<2%), and nonseparation of two lines, L_8 and L_{56}, in bands 27 and 39, respectively. In the first case, the products involved are in very small quantity, and the corresponding peaks are almost invisible in the FT absorption spectrum (that is the case, for example, for lines L_{42} and L_{57}). In the second case, two different products have almost the same resonance frequency (see Fig. 4), and thus could not be separated by any method. It may be noted that when two close peaks are not resolved, the intensity of the resulting peak corresponds roughly to the sum of the intensities of the theoretical lines (e.g., lines 7 and 8 in Table 4).

Concerning the 24 false detections, some explanations may be given. At first, 15 estimated lines are of extremely small amplitude (<1%), so that they may possibly be eliminated using an adequate threshold. Five of the 24 "false" lines, although having theoretically no existence, appear in the FT absorption spectrum. So it is possible that these lines correspond to impurities in the mixture considered. The last four false lines are actually artifacts caused by a bad estimation of the theoretical rank. This kind of phenomenon often occurs in the vicinity of lines with strong intensities. Fig. 4d shows three false lines estimated close to the resonant frequencies of the solvant.

The SB-HOYWSVD algorithm detected one line that was missed by the deconvolution (L_{62} on Table 4 and

Fig. 4). On the contrary, no lines detected by FT-MLD have been forgotten by the subband approach. It can be seen, for example, in Fig. 4b (band 37) that, around frequency 0.143, there are actually three components that are very close and overlapping. In such a situation, the deconvolution process is not easy and the amplitudes of the three peaks are badly estimated, while the proposed method performs much better (see Table 4). Note that the precision of frequency estimates is quite irreproachable. Concerning more particularly amplitude estimation, the mean relative errors observed with the two methods are comparable. Note the important errors made by the deconvolution method in the case of lines L_{38}, L_{39}, and L_{40}, when the SB-HOYWSVD method keeps a more reasonable behaviour. Calculation time was 3 min 13 s under the same conditions as before. It must be mentioned that, in general, it is possible to increase the number of correctly detected lines by using greater model orders, but this can lead to unacceptable false detection rates. For instance, with appropriate model orders, the method is able to detect 97 of the 104 lines but with a total of 138 detected lines.

5. Conclusion

The approach proposed in this paper increases considerably the applicability of LP-based methods. It allows one to process long FIDs made up of great numbers of damped sinusoids, with low model orders and thus with reduced complexity, although it makes use of the complete signal. Thus, the processing of FIDs of 128k samples takes no more than 3 or 4 min on a standard PC and under a Matlab environment. When compared to FT approaches, it has theoretical advantages because of its better statistical properties. The modeling process accounts for the presence of noise and, thanks to the subband decomposition, the estimation variance is maintained at a reasonable level. This allows, better performances at low SNR to be expected; thus it would be possible to reduce the number of accumulations. Moreover, when dealing with intricate spectra, our trials show that it performs comparably to a classical FT-MLD procedure in terms of frequency and amplitude estimates. But recall that, in practice, the deconvolution procedure requires the number of peaks to be chosen a priori. Here, the FT-MLD algorithm was used with the assumption of a perfectly known number of components. On the contrary, our approach is single-step, neither deconvolution nor numerical integration is necessary and the four parameters are given directly. In addition, its resolution capabilities are superior; thus it is able to increase the number of correctly detected lines. Note that the resolution capabilities depend strongly on the damping factor involved. It seems reasonable to expect a notable gain, comparatively to the FT, in the case of low damping factors. However, this improvement is sometimes achieved at the expense of a greater false detection rate. Fortunately, most of the false peaks may be suppressed with the help of an adapted threshold. This problem of false detections, which is related to the limited performances of the classical estimators of the number of components, may also be partly overcome by considering adaptive decomposition schemes.

Acknowledgments

The authors thank Dr. Henzel N. (IEPS Gliwice, Poland) and Pr. Nicole D. (UHP Nancy 1, France) for their advices and for having supplied us with the experimental signals.

References

[1] E.D. Laue, J. Skilling, J. Staunton, Maximum entropy reconstruction of spectra containing antiphase peaks, J. Magn. Reson. 63 (1985) 418–424.
[2] H. Barkhuijsen, R. de Beer, W.M.M.J. Bovée, D. van Ormondt, Retrieval of frequencies, amplitudes, damping factors, and phases from time-domain signals using a linear least-squares procedure, J. Magn. Reson. 63 (1985) 465–481.
[3] H. Gesmar, J.J. Led, Spectral estimation of complex time-domain NMR signals by linear prediction, J. Magn. Reson. 76 (1988) 183–192.
[4] D.S. Stephenson, Linear prediction and maximum entropy methods in NMR spectroscopy, Prog. NMR Spectr. 20 (1988) 515–626.
[5] J. Tang, J.R. Norris, Linear prediction z-transform (LPZ) method, Padé rational approximation, and the Burg maximum entropy extrapolation, J. Magn. Reson. 78 (1988) 23–30.
[6] P. Koehl, Linear prediction spectral analysis of NMR data, Prog. NMR Spectr. 34 (1999) 257–299.
[7] H. Barkhuijsen, R. de Beer, D. van Ormondt, Improved algorithm for noniterative time domain model fitting to exponentially damped magnetic resonance signals, J. Magn. Reson. 73 (1987) 553–557.
[8] W. Pijnappel, A. van den Boogaart, R. de Beer, D. van Ormondt, SVD-based quantification of magnetic resonance signals, J. Magn. Reson. 97 (1992) 122–134.
[9] S. van Huffel, H. Chen, C. Decaniere, P. van Hecke, Algorithm for time-domain NMR data fitting based on total least squares, J. Magn. Reson. Ser. A 110 (1994) 228–237.
[10] M.R. Wall, D. Neuhauser, Extraction, through filter-diagonalization, of general quantum eigenvalues or classical normal mode frequencies from a small number of residues or a short-time segment of a signal. I. Theory and application to a quantum-dynamics model, J. Chem. Phys. 102 (1995) 8011–8022.
[11] H. Hu, Q.N. Van, V.A. Mandelshtam, A.J. Shaka, Reference deconvolution, phase correction, and line listing of NMR spectra by the 1D filter diagonalization method, J. Magn. Reson. 134 (1998) 76–87.
[12] O. Caspary, M. Tomczak, P. Nus, P. Staiquly, DSP-based AR spectral estimation with zoom effect for NMR spectroscopy, in: Proc. IEEE Instrum. Measur. Techn. Int. Conf., 1993, pp. 128–131.
[13] N. Henzel, M. Tomczak, D. Brie, D. Nicole, Comparaison d'estimateurs spectraux appliqués à la spectroscopie RMN ^{13}C, in:

Proc. 14th Colloque GRETSI, vol. 2, Juan-les-Pins, France, 1993, pp. 1295–1298.
[14] M.P. Quirk, B. Liu, Improving resolution for autoregressive spectral estimation by decimation, IEEE Trans. Acoust. Speech Signal Process. 31 (1983) 630–637.
[15] S. Rao, W. Pearlman, Analysis of linear prediction, coding, and spectral estimation from subbands, IEEE Trans. Inform. Theory 42 (1996) 1160–1178.
[16] J. Tang, J.R. Norris, LP-ZOOM, a linear prediction method for local spectral analysis of NMR signals, J. Magn. Reson. 79 (1988) 190–196.
[17] A.R. Mazzeo, M.A. Delsuc, A. Kumar, G.C. Levy, Generalized maximum entropy deconvolution of spectral segments, J. Magn. Reson. 81 (1989) 512–519.
[18] V.A. Mandelshtam, H.S. Taylor, A.J. Shaka, Application of the filter diagonalization method to one- and two-dimensional NMR spectra, J. Magn. Reson. 133 (1998) 304–312.
[19] H. Gesmar, P.C. Hansen, Fast linear prediction and its application to NMR spectroscopy, J. Magn. Reson. Ser. A 106 (1994) 236–240.
[20] P. Stoica, T. Söderström, High-order Yule–Walker equations for estimating sinusoidal frequencies: the complete set of solutions, Signal Process. 20 (1990) 257–263.
[21] S.L. Marple, Digital Spectral Analysis with Applications, Prentice-Hall, Englewood Cliffs, NJ, 1987.
[22] S.M. Kay, Modern Spectral Estimation. Theory and Application, Prentice-Hall, Englewood Cliffs, NJ, 1988.
[23] P. Händel, High-order Yule–Walker estimation of the parameters of exponentially damped cisoids in noise, Signal Process. 32 (1993) 315–328.
[24] D. Brie, D. Dal Ponte, M. Tomczak, A. Richard, Estimation of the order of the AR part of ARMA models with application to frequency estimation, in: M. Holt, C. Cowan, P. Grant, W. Sandham (Eds.), Signal Processing VII: Theories and Applications, European Association for Signal Processing, 1994, pp. 664–667.
[25] P. Stoica, R.L. Moses, T. Söderström, J. Li, Optimal HOYW estimation of sinusoidal frequencies, IEEE Trans. Signal Process. 39 (1991) 1360–1368.
[26] B. Friedlander, The overdetermined recursive instrumental variable method, IEEE Trans. Au. Con. 29 (1984) 353–356.
[27] G.E.P. Box, G.M. Jenkins, Time Series Analysis. Forecasting and Control, Holden-Day, Oakland, 1976.
[28] D.W. Tufts, R. Kumaresan, Estimation of frequencies of multiple sinusoids: making linear prediction perform like maximum likelihood, Proc. IEEE 70 (1982) 975–989.
[29] B. Friedlander, B. Porat, The modified Yule–Walker method of ARMA spectral estimation, IEEE Trans. Aerosp. Elect. Syst. 20 (1984) 158–173.
[30] M. Wax, T. Kailath, Detection of signals by information theoretic criteria, IEEE Trans. Acoust. Speech Signal Process. 33 (1985) 387–392.
[31] V.U. Reddy, L.S. Biradar, SVD-based information theoretic criteria for detection of the number of damped/undamped sinusoids and their performance analysis, IEEE Trans. Signal Process. 41 (1993) 2872–2881.
[32] R. Kumaresan, D.W. Tufts, Estimating the parameters of exponentially damped sinusoids and pole-zero modeling in noise, IEEE Trans. Acoust. Speech Signal Process. 30 (1982) 833–840.
[33] D. Dal Ponte, D. Brie, M. Tomczak, A. Richard, Order determination for the HOYW estimator, in: Proc. 12th Europ. Conf. on Circuits. Theor. Design, Istanbul, Turkey, vol. 1, 1995, pp. 119–122.
[34] P.P. Vaidyanathan, Multirate Systems and Filter Banks, Prentice-Hall, Englewood Cliffs, NJ, 1993.
[35] W.M. Steedly, C.-H.J. Ying, R.L. Moses, A modified TLS-Prony method using data decimation, IEEE Trans. Signal Process. 42 (1994) 2292–2303.
[36] C. van den Branden Lambrecht, M. Karrakchou, Wavelet packets for the estimation of parameters of localized sinusoids, in: M. Holt, C. Cowan, P. Grant, W. Sandham (Eds.), Signal Processing VII: Theories and Applications, European Association for Signal Processing, 1994, pp. 653–656.
[37] J. Chen, A.J. Shaka, V.A. Mandelshtam, RRT: The regularized resolvent transform for high-resolution spectral estimation, J. Magn. Reson. 147 (2000) 129–137.
[38] A. Benyassine, A. Akansu, Subspectral modeling in filter banks, IEEE Trans. Signal Process. 43 (1995) 3050–3053.
[39] L.K. Denoyer, J.G. Dodd, Maximum likelihood deconvolution for spectroscopy and chromatography, Am. Lab. 23 (1991) 19–22.